Improved Sliding Mode and PLL Speed Estimators for Sensorless Vector Control of Induction Motors

Diego D. Pinheiro, Emerson G. Carati, Felipe S. Del Sant, Jean P. da Costa, Rafael Cardoso, Carlos M. de P. Stein
PPGEE – Postgraduate Program in Electrical Engineering
UTFPR – Federal University of Technology - Paraná
Pato Branco, Brazil
diego.npn@gmail.com, emerson@utfpr.edu.br, felipesant@gmail.com, jpcosta@utfpr.edu.br, rcardoso@utfpr.edu.br, cmstein@utfpr.edu.br

***Abstract*— In the last four decades, several approaches of sensorless drives for induction machines (SDIM) have been proposed. This paper presents an evaluation and improvement of conventional and high performance techniques for rotor speed estimation. The proposed SDIM uses indirect field-oriented control (IFOC), which is composed of proportional-integral type (PI) controllers. The speed estimation techniques analyzed are Rotor Flux MRAS, Back EMF MRAS, and Instantaneous Reactive Power MRAS, PLL and Sliding Mode. This paper also shows improvements at structure of sliding mode estimator. The techniques are evaluated using numerical and experimental results. The setup applied a F28069 DSP for experimental implementation of the control scheme and the speed estimation techniques. The performance verification considered a wide speed range and load changes. Results demonstrates the feasibility of replacing mechanical sensors by analyzed estimation techniques.**

Keywords — Electric motor drives, induction motor, speed estimation, sensorless techniques, vector control.

I. INTRODUCTION

Induction Motor (IM) have been widely used in the movable portion of industrial controls. The high performance control methods are based on the concept of direct field-oriented (DFOC) or indirect field-oriented (IFOC) [1]. According to Castaldi et al. [1] IFOC is one of the most effective vector control techniques for IM due to the simplicity of design and implementation, resulting in a good torque and speed performance system.

Speed information is required for the operation of vector-controlled IM drive. The rotor speed can measured through a mechanical sensor or can be estimated using voltage, current signals, and machine parameters. Speed estimation is an issue of particular interest with IM drives where the mechanical speed of the rotor is generally different from the speed of the revolving magnetic field. The advantages of speed sensorless IM are reduce hardware complexity and lower cost, reduce size of the drive machine, elimination of the sensor cable, better noise immunity, increased reliability and less maintenance requirements [2], [3].

Different solutions for sensorless AC drives have been proposed in the past few decades. Various speed estimation algorithms and speed sensorless control methods have been reported in literature as Model Reference Adaptive System (MRAS) [4]-[8], Phase-Locked Loop (PLL) [9]-[13] and sliding mode [14]-[19].

Model Reference Adaptive System (MRAS) is one of the traditional speed observers usually applied for sensorless IM drives. MRAS speed observers usually applies two models: a *reference model* and an *adjustable model.* The speed is estimated from model outputs, like rotor fluxes, back EMF or instantaneous reactive power, where one model is a function of speed while the other model is speed independent. The rotor speed is obtained by means of an adaptation mechanism, which considers the difference between the two estimated values. The adaptation mechanism adjusts the adaptive model until the difference between the outputs of the two models becomes small enough. However, the performance of the system is usually affected by parameter variations and it is not satisfactory close to zero speed [4]-[8].

The rotor flux angle also can be estimated with a Phase Locked Loop (PLL) [13] and Sliding mode observers [16]-[18]. The PLL synthesizes a rotating reference frame that always tries instantaneously to align with the voltage vector of the machine. The PLL only uses the voltage or current vector and is likely to yield a better frequency estimate under real conditions (offsets, imperfections, parameter variations, etc.) than the methods based on the machine models. Sliding Mode Observer (SMO) is another of the prospective methodologies for electrical machines estimation, due to its order reduction, disturbance rejection, strong robustness, and simple implementation by means of power converter. These advantages can be employed for position and speed control of high performance AC drives.

This paper presents an evaluation of main speed estimation techniques for IM drives. The mathematical models of the estimators are presented and their efficiency is evaluated by both simulation and experiments. The main contribution of this paper is to propose improvements in the structure of the sliding mode observer to obtain the rotor speed, based on the stator current and rotor fluxes.

II. DYNAMIC MODELLING OF INDUCTION MACHINE

The model of the induction motor in the rotational reference frame is obtained by transforming the dynamic equations of the fluxes and currents from the stationary reference frame to the rotating frame aligned with the rotor flux. The model is given as

$$\begin{cases} \mathbf{v_s} = R_s \mathbf{i_s} + \sigma L_s \dfrac{d\mathbf{i_s}}{dt} + \dfrac{M}{L_r}\dfrac{d\boldsymbol{\lambda}_\mathbf{r}}{dt} + j\sigma L_s \omega \mathbf{i_s} + j\dfrac{M}{L_r}\omega\boldsymbol{\lambda}_\mathbf{r} \\ 0 = \dfrac{1}{T_r}\boldsymbol{\lambda}_\mathbf{r} - \dfrac{M}{T_r}\mathbf{i_s} + \dfrac{d\boldsymbol{\lambda}_\mathbf{r}}{dt} + j\omega_r \boldsymbol{\lambda}_\mathbf{r} \end{cases} \quad (1)$$

The motion equation is

$$\Gamma_e - \Gamma_l = J\frac{d\omega_r}{dt} + D\omega_r, \tag{2}$$

where the electromagnetic torque is

$$\Gamma_e = \frac{3P}{4}\frac{M}{L_r}\left(\lambda_{dr} i_{qs} - \lambda_{qr} i_{ds}\right). \tag{3}$$

Assume that the load torque and viscous coefficient are unknown, such $\Gamma = \Gamma_l + D\omega_r$, so (3) can be written as

$$\Gamma_e - \Gamma = J\frac{d\omega_r}{dt}. \tag{4}$$

The aforementioned variables are given as: R_s, R_r, are stator and rotor resistances; L_s, L_r are the stator and rotor inductances; M is the magnetizing inductance; $T_r = L_r/R_r$ is the rotor time constant; $\sigma = 1 - L_m^2/L_sL_r$ is the leakage coefficient; $\boldsymbol{\lambda}_s = [\lambda_{ds}\ \lambda_{ds}]$ and $\boldsymbol{\lambda}_r = [\lambda_{dr}\ \lambda_{dr}]$ are the stator and rotor fluxes; $\boldsymbol{v}_s = [v_{ds}\ v_{qs}]$ are the stator voltages; $\mathbf{i}_s = [i_{ds}\ i_{qs}]$ and $\mathbf{i}_r = [i_{dr}\ i_{qr}]$ are the stator and rotor currents; ω_r is the angular rotor speed; ω is the angular speed of the reference frame; Γ_e is the electromagnetic torque; Γ_l is the load torque; J is the rotor inertia; D is the viscous friction coefficient; and, P is the number of poles.

III. Indirect Field Oriented Control

The main objective of the field orientation of induction motors is to control the torque and the flux independently, as in DC machine control. This is done by using *d-q* rotating reference frame synchronously with the rotor flux space vector and aligning it with the d-axis such $\lambda_{dr} = \lambda$ and $\lambda_{qr} = 0$. Then, the torque in (3) may be rewritten as follows:

$$\Gamma_e = k\lambda_r i_{qs} \tag{5}$$

where $k = PM/L_r$. So, i_{qs} can be used as the input command of the torque or active power, whereas i_{ds} is used for machine magnetization or reactive power.

Considering the IM electric model referenced to the rotor flux and the system as in [19], Fig. 1 presents the IFOC control structure used to perform current and voltage machine driving for a given speed reference and flux reference. The variables with $(^*)$ are input commands.

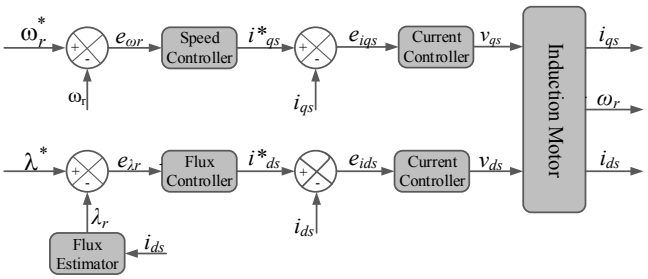

Fig. 1. IFOC control structure for induction motors.

From the input variable ω_r^* and λ^*, the IFOC approach uses four PI controllers to generate output voltages v_{ds} and v_{qs}, which are used to drive the motor using PWM modulation. As it shown in Fig. 1, the control loops uses feedback from motor currents, estimated flux and rotor speed. The continuous-time transfer function of the PI controllers from error signal $E(s)$ to controller output $Y(s)$ is given by

$$\frac{Y(s)}{E(s)} = K_p + \frac{K_i}{s}. \tag{6}$$

In order to obtain a discrete time recursive equation the Backward Euler's Method is used. So, the flux, speed and currents equations for the PI discrete-time controllers are written as

$$y[k] = y[k-1] + \left(K_p + K_iT_s\right)e[k] - K_p e[k-1]. \tag{7}$$

The IFOC uses the rotor flux estimation based on the mathematical model of the IM and it allows the motor to operate with different load and speed profiles. In conventional approaches, the flux input is the rated one. The rotor flux λ_{dr} is estimated from measured current i_{ds} as

$$\frac{d\lambda_{dr}}{dt} = \frac{MR_r}{L_r} i_{ds} - \frac{R_r}{L_r}\lambda_{dr}. \tag{8}$$

The rotor flux speed ω used in synchronous transformation is estimated from

$$\omega = \omega_r + \frac{MR_r}{L_r}\frac{i_{qs}}{\lambda_{dr}^*}. \tag{9}$$

IV. Speed Sensorless Algorithms

In recent years, several sensorless vector control schemes [4]-[19] have been proposed to obtain the rotor speed of induction motors. However, several techniques have estimation issues at low speed or intolerance to parameters variation. The aim of this work is to discuss and propose high performance sensorless techniques such electric drives can operate without the use of mechanical sensors. In this way, the following techniques are evaluated: MRAS, PLL and SMO. Moreover, SMO improvements are proposed and investigated in order to reduce chattering and error in estimated speed.

A. MRAS Based on Back-EMF

The MRAS speed estimation is one of the most used techniques for speed estimation. Its structure consists of a reference model, an adjustable model and an adaptive mechanism, as shown in Fig. 2. The reference model is independent of the rotor speed and it is used to calculate the state variable $\mathbf{x}$, from the terminal voltages and currents. The adjustable model estimates the state variable $\hat{\mathbf{x}}$ and it is rotor speed dependent. The error ε between both set of state variables is then used to drive an adaptation mechanism that generates the estimated speed $\hat{\omega}_r$ for the adjustable model. It should be noted that speed estimation methods using MRAS can be classified into various types according to the state variable. The most commonly used technique are the rotor Flux based MRAS, Back Electromotive Force based MRAS and Instantaneous Reactive Power based MRAS. In this

work, EMF-based MRAS is used, since it presents reduced speed error and smaller parametric dependence.

The Back EMF scheme follows the approach presented in [6]. IM equations can be expressed in the stationary frame as

$$\mathbf{v_s} = R_s \mathbf{i_s} + \sigma L_s \frac{d\mathbf{i_s}}{dt} + \mathbf{e_m}. \tag{10}$$

Isolating $\mathbf{e_m}$ term in (10) leads to the reference model for back-EMF

$$\hat{\mathbf{e}}_{\mathbf{m}1} = \mathbf{v_s} - \left(R_s \mathbf{i_s} + \sigma L_s \frac{d\mathbf{i_s}}{dt} \right). \tag{11}$$

From of IM model (1), $d(\mathbf{i_m})/dt$ is obtained as

$$\frac{d\mathbf{i_m}}{dt} = \hat{\omega}_r \otimes \mathbf{i_m} - \frac{1}{T_r}\mathbf{i_m} + \frac{1}{T_r}\mathbf{i_s}, \tag{12}$$

where $\mathbf{i_m} = \mathbf{i_s} + \mathbf{i_r}\, L_r / M$, is the magnetizing current vector. The back-EMF adaptive model can be obtained as

$$\hat{\mathbf{e}}_{\mathbf{m}2} = \left(\frac{M^2}{L_r} \right) \frac{d\mathbf{i_m}}{dt} = \frac{M^2}{L_r} \left(\hat{\omega}_r \otimes \mathbf{i_m} - \frac{1}{T_r}\mathbf{i_m} + \frac{1}{T_r}\mathbf{i_s} \right) \tag{13}$$

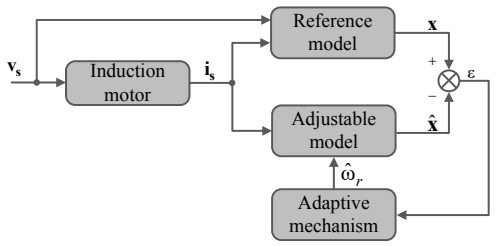

Fig. 2. Speed estimation approach using MRAS

Two independent observers are applied to estimate the back-EMF vector. While (13) is $\hat{\omega}_r$ dependent, (11) is obtained from stator voltages and currents. The error between the outputs of the two observers is then used by the adaptive scheme to generate the $\hat{\omega}_r$ estimative, as follows:

$$\hat{\omega}_r = \left(K_p + \frac{K_i}{s} \right) \left(\hat{\mathbf{e}}_{\mathbf{m}1} \otimes \hat{\mathbf{e}}_{\mathbf{m}2} \right) \tag{14}$$

This MRAS scheme does not require pure integrators in their reference models, but it can be affected by stator resistance variations due to temperature changes.

B. Phase-Locked Loop

The block diagram of synchronous frequency estimator based on PLL theory is shown in Fig. 3.

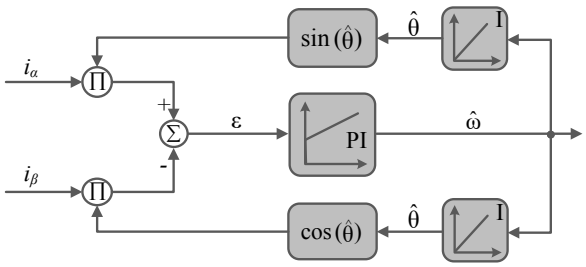

Fig. 3. Synchronous estimation based on PLL.

From Fig. 3, the input error ε can be obtained as

$$\varepsilon = i_{\alpha s} \sin\left(\hat{\theta}\right) + i_{\beta s} \cos\left(\hat{\theta}\right) = i_s \sin\left(\theta - \hat{\theta}\right) \tag{15}$$

where $i_s = \sqrt{i_{\alpha s} + i_{\beta s}}$.

When $\tilde{\theta} = \theta - \hat{\theta}$ is small the error ε can be linearized as

$$\varepsilon = i_s \sin(\theta - \hat{\theta}) \approx i_s (\theta - \hat{\theta}) \approx i_s \tilde{\theta}. \tag{16}$$

Assuming that ε is calculated correctly, from Fig. 3 the speed estimation can be obtained as

$$\frac{d\hat{\omega}}{dt} = \kappa_1 K \tilde{\theta}, \text{ and } \frac{d\hat{\theta}}{dt} = \hat{\omega} + \kappa_2 K \tilde{\theta}. \tag{17}$$

where κ_1 is the integral gain and κ_2 is the proportional gain of the PI controller. As in Eskola [25], using the linearized equation (16) the transfer function can be written as:

$$\frac{\hat{\omega}(s)}{\omega(s)} = \frac{\kappa_2 K s + \kappa_1 K}{s^2 + \kappa_2 K s + \kappa_1 K}. \tag{18}$$

The expression (18) is the transfer function of Fig.3. This equation has a characteristic polynomial $s^2+2\rho s+\rho^2$. For the correct choice of the gains κ_1 and κ_2, obtaining satisfactory performance and avoiding oscillations, both poles must be located on the real axis [12] such $s = -\rho$, with ρ as a positive constant. The gains κ_1 and κ_2 can be obtained according to Eskola [20], where K is scale factor:

$$\kappa_1 = \frac{\rho^2}{K} \quad \text{and} \quad \kappa_2 = \frac{2\rho}{K}. \tag{19}$$

A more detailed analysis of gains and stability analysis of the PLL scheme applied to the motor control is carried out by Harnefors et al. [12]. To obtain the rotor speed using the equation machine model, according to

$$\hat{\omega}_r = \frac{1}{2P} \left(\hat{\omega} - \frac{M}{T_r} \frac{i_{qs}}{\lambda_{dr}} \right). \tag{20}$$

C. Sliding Mode Observer

In general, sliding mode observers are estimators that uses input variables defined by discontinuous functions of the error from the estimated and measured outputs. The system reconstruction rate can be achieved by enforcing sliding mode.

1) Conventional Sliding Mode

As it is well known, from sliding mode controllers, the system's dynamic behavior in the sliding mode is only decided by the chosen surfaces in the state space and is not affected by the matched uncertainly [18]. Fortunately, these well-known advantages of sliding mode control methodology such as order reduction, disturbance rejection, and strong robustness may be inherited in sliding mode observers.

The model of the squirrel-cage induction machine can be expressed in the state space representation $\dot{\mathbf{x}} = \mathbf{A}\mathbf{x} + \mathbf{B}\mathbf{u}$

considering the stator-current and rotor-flux components of the *dq* system as

$$\begin{bmatrix} \dot{\bar{\mathbf{i}}}_{\mathbf{s}} \\ \dot{\bar{\boldsymbol{\lambda}}}_{\mathbf{r}} \end{bmatrix} = \begin{bmatrix} \mathbf{A_{11}} & \mathbf{A_{12}} \\ \mathbf{A_{21}} & \mathbf{A_{22}} \end{bmatrix} \begin{bmatrix} \bar{\mathbf{i}}_{\mathbf{s}} \\ \bar{\boldsymbol{\lambda}}_{\mathbf{r}} \end{bmatrix} + \begin{bmatrix} \mathbf{B_1} \\ 0 \end{bmatrix} \begin{bmatrix} \bar{\mathbf{v}}_{\mathbf{s}} \end{bmatrix} \tag{21}$$

where $\mathbf{A_{11}}=a\mathbf{I}$, $\mathbf{A_{12}}=c\mathbf{I}+d\mathbf{J}$, $\mathbf{A_{21}}=e\mathbf{I}$, $\mathbf{A_{22}}=-\varepsilon\mathbf{A_{12}}$, $\mathbf{B_1}=b_1\mathbf{I}$, and $\mathbf{I}=\begin{bmatrix}1 & 0\\ 0 & 1\end{bmatrix}$, $\mathbf{J}=\begin{bmatrix}0 & -1\\ 1 & 0\end{bmatrix}$, $a=-\left(\frac{R_s}{\sigma L_s}+\frac{M}{\sigma L_s T_r L_r}\right)$, $b_1=\frac{1}{\sigma L_s}$, $c=\frac{1}{\varepsilon T_r}$, $d=\frac{\hat{\omega}_r}{\varepsilon}$, $e=\frac{M}{T_r}$, $\varepsilon=\frac{\sigma L_s L_r}{M}$.

As shown in Fig.4.(a), a sliding mode observer for rotor flux and stator-current along with a sliding mode speed estimation are shown working parallel to each other.

From the IM model and considering the stator currents as the system outputs, a sliding mode observer for rotor flux estimation can be constructed as

$$\frac{d\hat{\mathbf{x}}}{dt} = \mathbf{A}\hat{\mathbf{x}} + \mathbf{B}\mathbf{v}_{\mathbf{s}} + \mathbf{K}\,\mathrm{sgn}\left(\hat{\mathbf{i}}_{\mathbf{s}} - \mathbf{i}_{\mathbf{s}}\right) \tag{22}$$

where $\mathbf{K}$ is a gain matrix which can be arranged in the general form $\mathbf{K}=\begin{bmatrix}K_1 & -K_1\end{bmatrix}^T, K_1 = k\mathbf{I}$ and k is the switching gain.

The error equation takes in account the parameter variation and it can be expressed by subtracting (21) from (22):

$$\frac{d\mathbf{e}}{dt} = \mathbf{A}\mathbf{e} + \Delta\mathbf{A}\hat{\mathbf{x}} + \mathbf{K}\,\mathrm{sgn}\left(\hat{\mathbf{i}}_{\mathbf{s}} - \mathbf{i}_{\mathbf{s}}\right) \tag{23}$$

where $\mathbf{e}=\hat{\mathbf{x}}-\mathbf{x}=\begin{bmatrix}\mathbf{e}_{\mathbf{i}} & \mathbf{e}_{\boldsymbol{\lambda}}\end{bmatrix}^T$, $\mathbf{e_i}=\hat{\mathbf{i}}_{\mathbf{s}}-\mathbf{i}_{\mathbf{s}}$, $\mathbf{e}_{\boldsymbol{\lambda}}=\hat{\boldsymbol{\lambda}}_{\mathbf{r}}-\boldsymbol{\lambda}_{\mathbf{r}}$ and $\Delta\mathbf{A}=\begin{bmatrix}\Delta\mathbf{A}_{11} & \Delta\mathbf{A}_{12}\\ \Delta\mathbf{A}_{21} & \Delta\mathbf{A}_{22}\end{bmatrix}$.

The sliding mode concept can be applied to the stator current defining the sliding surface as

$$\mathbf{e_i} = \hat{\mathbf{i}}_{\mathbf{s}} - \mathbf{i}_{\mathbf{s}} = 0\,. \tag{24}$$

The sliding mode occurs when the sliding condition is satisfied.

$$\frac{d\mathbf{e}_{\mathbf{i}}}{dt}\cdot\mathbf{e}_i^T < 0 \tag{25}$$

Considering that this condition is satisfied, with a small switching gain k, from (25) follows

$$\frac{d\mathbf{e}_{\mathbf{i}}}{dt} = \mathbf{e}_i^T = 0\,. \tag{26}$$

Using (24) it results

$$0 = \mathbf{A_{12}}\mathbf{e}_{\boldsymbol{\lambda}} + \Delta\mathbf{A_{11}}\hat{\mathbf{i}}_{\mathbf{s}} + \Delta\mathbf{A_{11}}\hat{\boldsymbol{\lambda}} - \boldsymbol{\upsilon} \tag{27}$$

and

$$\frac{d\mathbf{e}_{\boldsymbol{\lambda}}}{dt} = \mathbf{A_{22}}\mathbf{e}_{\boldsymbol{\lambda}} + \Delta\mathbf{A_{21}}\hat{\mathbf{i}}_{\mathbf{s}} + \Delta\mathbf{A_{22}}\hat{\boldsymbol{\lambda}}_{\mathbf{r}} + \boldsymbol{\upsilon} \tag{28}$$

where, $\boldsymbol{\upsilon} = -\mathbf{K_1}\,\mathrm{sgn}\left(\hat{\mathbf{i}}_{\mathbf{s}} - \mathbf{i}_{\mathbf{s}}\right)$.

From (27) and (28), the error equation for the rotor flux in sliding mode condition is obtained as

$$\frac{d\mathbf{e}_{\boldsymbol{\lambda}}}{dt} = \left(\mathbf{A_{22}} + \mathbf{A_{12}}\right)\mathbf{e}_{\boldsymbol{\lambda}} + \left(\Delta\mathbf{A_{21}} + \Delta\mathbf{A_{11}}\right)\hat{\mathbf{i}}_{\mathbf{s}} + \\ + \left(\Delta\mathbf{A_{22}} + \Delta\mathbf{A_{12}}\right)\hat{\boldsymbol{\lambda}}_{\mathbf{r}} \tag{29}$$

If the rotor speed is a varying parameter and assuming no other parameter variations, the terms of the $\Delta\mathbf{A}$ matrix are specified as

$$\Delta\mathbf{A_{11}} = 0, \Delta\mathbf{A_{12}} = \frac{-\Delta\omega_r\mathbf{J}}{\varepsilon}, \Delta\mathbf{A_{21}} = 0, \\ \Delta\mathbf{A_{22}} = \Delta\omega_r\mathbf{J}, \Delta\omega_r = \hat{\omega}_r - \omega_r. \tag{30}$$

From (29) and (30), the error equation of the rotor flux observer in sliding mode condition is obtained as

$$\frac{d\mathbf{e}_{\boldsymbol{\lambda}}}{dt} = \left(\mathbf{A_{22}} + \mathbf{A_{12}}\right)\mathbf{e}_{\boldsymbol{\lambda}} + \left(\mathbf{I} - \frac{\mathbf{I}}{\varepsilon}\right)\mathbf{J}\Delta\omega_r\hat{\boldsymbol{\lambda}}_{\mathbf{r}}\,. \tag{31}$$

For the stability analysis and design of the sliding mode observer, a Lyapunov function candidate is chosen considering the flux estimation error and speed estimation error:

$$V = \mathbf{e}_{\boldsymbol{\lambda}}^T\mathbf{e}_{\boldsymbol{\lambda}} + \frac{1}{\mu\varepsilon}\Delta\omega_r^2, \qquad \mu > 0\,. \tag{32}$$

If (32) is positive definite and its time derivative is negative definite, the estimator is stable and estimation error converges to zero asymptotically. The time derivative of V can be expressed as

$$\dot{V} = \dot{V}_1 + \dot{V}_2 \tag{33}$$

where

$$\dot{V}_1 = \boldsymbol{\upsilon}^T\boldsymbol{\Lambda}^T\mathbf{A_{12}^{-1}}\boldsymbol{\upsilon} \tag{34}$$

$$\dot{V}_2 = \boldsymbol{\upsilon}^T\boldsymbol{\Lambda}^T\mathbf{A_{12}^{-1}}\frac{\Delta\omega_r}{\varepsilon}\mathbf{J}\hat{\boldsymbol{\lambda}}_{\mathbf{r}} + \frac{2}{\mu\varepsilon}\Delta\omega_r\frac{d}{dt}\hat{\omega}_r \tag{35}$$

and $\boldsymbol{\Lambda} = \mathbf{I} - \varepsilon\mathbf{I}$.

The expression (33) will be negative definite if $\dot{V}_1 < 0$ and $\dot{V}_2 = 0$. The condition $\dot{V}_1 < 0$ is satisfied by choosing

$$\boldsymbol{\Lambda}^{\mathrm{T}} = -\gamma\mathbf{A_{12}}, \qquad \gamma > 0 \tag{36}$$

From this assumption, the condition $\dot{V}_2 = 0$ results

$$\frac{d\hat{\omega}_r}{dt} = \mu\gamma\boldsymbol{\upsilon}^T\mathbf{J}\hat{\boldsymbol{\lambda}}_{\mathbf{r}}. \tag{37}$$

This equation can be rewritten for the speed estimation as

$$\frac{d\hat{\omega}_r}{dt} = \mu\gamma\left[k\,\mathrm{sgn}\left(\hat{i}_{ds} - i_{ds}\right)\hat{\lambda}_{qr} - k\,\mathrm{sgn}\left(\hat{i}_{qs} - i_{qs}\right)\hat{\lambda}_{dr}\right] \tag{38}$$

2) Improved Sliding Mode

From the above approach, an improved observer structure that also applies sliding mode concept is now

introduced to estimate the rotor speed. This structure differs from the conventional one with respect to obtaining rotor flux variable. In this case, the flux model considers the stator currents and motor parameters to produce the rotor flux estimative. The fluxes equations are

$$\boldsymbol{\lambda}_{\mathbf{s}} = L_s \mathbf{i}_{\mathbf{s}} + M \mathbf{i}_{\mathbf{r}}, \tag{39}$$

$$\boldsymbol{\lambda}_{\mathbf{r}} = L_r \mathbf{i}_{\mathbf{r}} + M \mathbf{i}_{\mathbf{s}}. \tag{40}$$

From (40), isolating the rotor currents, it can be rewritten as

$$\mathbf{i}_{\mathbf{r}} = \frac{\boldsymbol{\lambda}_{\mathbf{r}}}{L_r} + \frac{M}{L_r}\mathbf{i}_{\mathbf{s}}. \tag{41}$$

Substituting (41) into (39), it results

$$\boldsymbol{\lambda}_{\mathbf{s}} = L_s \mathbf{i}_{\mathbf{s}} + M\left(\frac{\boldsymbol{\lambda}_{\mathbf{r}}}{L_r} - \frac{M}{L_r}\mathbf{i}_{\mathbf{s}}\right), \tag{42}$$

and rearranging (51), it gives

$$\boldsymbol{\lambda}_{\mathbf{s}} = \sigma L_s \mathbf{i}_{\mathbf{s}} + \frac{M}{L_r}\boldsymbol{\lambda}_{\mathbf{r}}. \tag{43}$$

The TIM stator voltages can be described by

$$\mathbf{v}_{\mathbf{s}} = R_s \mathbf{i}_{\mathbf{s}} + \frac{d\boldsymbol{\lambda}_{\mathbf{s}}}{dt}. \tag{44}$$

Noting that $\omega = 0$ in the stationary reference frame system, from (43) and (44) the stator voltage can be rewritten as

$$\mathbf{v}_{\mathbf{s}} = R_s \mathbf{i}_{\mathbf{s}} + \frac{d}{dt}\left(\sigma L_s \mathbf{i}_{\mathbf{s}} + \frac{M}{L_r}\boldsymbol{\lambda}_{\mathbf{r}}\right) \tag{45}$$

From (45), the rotor flux expression can be obtained as function of the voltage and current stator variables, i.e.,

$$\frac{d\boldsymbol{\lambda}_{\mathbf{r}}}{dt} = \frac{L_r}{M}\left(\mathbf{v}_{\mathbf{s}} - R_s \mathbf{i}_{\mathbf{s}} - \sigma L_s \frac{d\mathbf{i}_{\mathbf{s}}}{dt}\right). \tag{46}$$

From (22), (38) and (46), Fig. 4(b) shows the structure for estimation of rotor speed on the rotor flux obtained through the stator variables.

There are two points worthwhile to be noted in the proposed sensorless control scheme for IM:

- The design of the sliding mode controller and observer is carried out as an unified approach, instead of isolated as it is usually performed in conventional observer design methods;
- In the system analysis, it considers the advantage of the order reduction of sliding mode approach. Although the flux/speed observer is a fourth order system, the errors e_λ and e_i of the sliding mode observer turns in a second order system after the sliding mode surface is obtained. The order reduction is very helpful for the stability analysis of the nonlinear time-varying error system.

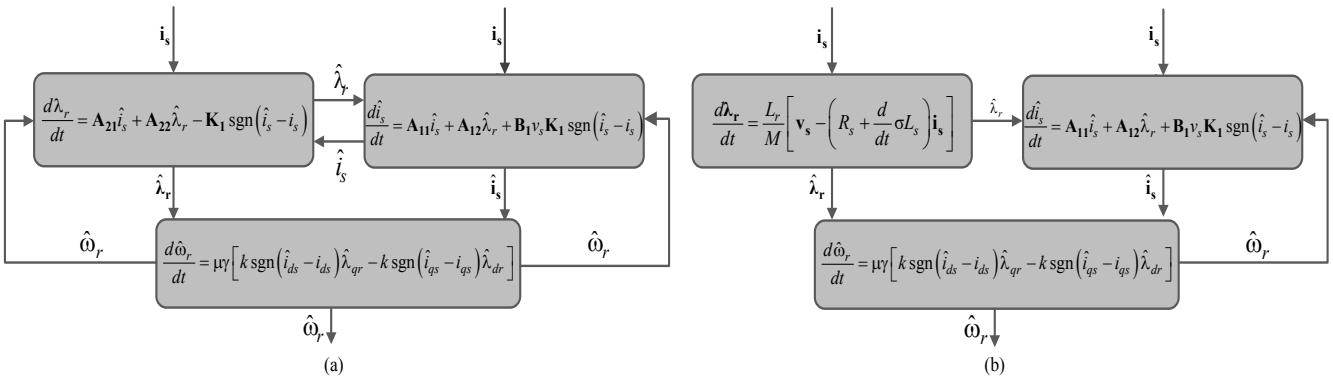

Fig. 4. Block diagram sliding mode observer to speed estimators: (a) Conventional sliding mode observer and (b) Improved sliding mode observer

In this scheme, instead of use of another sliding mode expression, the rotor flux is directly obtained from stator currents and controller output stator voltages. The main drawback of this scheme is that the rotor flux depends on the motor parameters and so it can be sensitive to resistance variation.

V. Numerical Analysis

The numerical evaluation of the different schemes for the sensorless position vector control considered takes in account the motor model described in (1)-(4) and IFOC control scheme (5)-(10), which were simulated with 6 kHz sampling time using Matlab environment. The nominal parameters of the experimental evaluation machine are used for the IM in numerical analysis. Table I presents the parameters of the numerical and experimental induction machine, where ω_n is rated angular speed, V_n is rated voltage, I_n is rated current and P_n is rated power.

TABLE I
IM Parameters

P_n	3 HP	L_{ls}	*0.0073 H*
V_n	220 V	L_{lr}	*0.0073 H*
P	4 poles	L_M	*0.1631 H*
I_n	11.1 A	R_r	*1.25* Ω
D	*0.02 Nm.s/rad*	R_s	*1.72* Ω
ω_n	1715 rpm	J	*0.0105 kg.m²*

Figures 5-8 presents results obtained from numerical analysis. Fig. 5 shows the IFOC performance for speed control and the respective behavior of stator-currents in the *d-q* system. In this case, the rated flux reference is used for simulation. It can be observed that i_{ds} current remains practically constant to ensure rotor flux close to nominal while i_{qs} varies according to the required torque/speed.

The rotor speed estimation schemes are evaluated in the same test conditions. Since the back-EMF presents better

dynamic performance compared with other MRAS schemes, other MRAS results are omitted here.

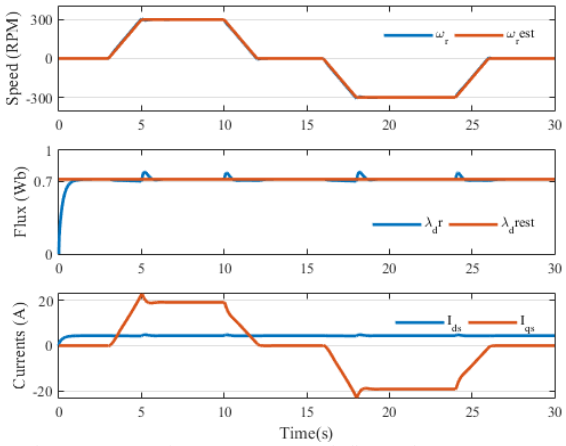

Fig. 5. IFOC perfomance - IM speed, flux and stator currents.

Figure 6 shows the rotor speed and its estimative speed for different speed reference levels using the following techniques: MRAS back-EMF, PLL, conventional sliding mode observer (CSMO) and improved sliding mode observer (ISMO). It can be seen that in nominal case the four techniques have good speed estimation performance, however the CSMO has higher estimation ripple due to its quasi-sliding mode behavior.

Figure 7 evaluates the performance of the estimation techniques rotor speed with 5Nm load torque at 5s, The load is increased to 10Nm at 10s and it decreases to 5Nm and 0Nm, at 15s and 20s, respectively. The MRAS technique shows lower absolute errors for nominal IM parameters.

The evaluation of estimation techniques considering IM parametric variation is presented in Fig. 8, considering the scenarios presented in Table II. In this case the MRAS and Sliding Mode based techniques present high errors due to rotor resistance variation. Even with significant resistance and inductance variation the PLL technique remains practically insensitive to any parameter variation.

TABLE II
Estimators sensitivity due parameters variation

IM Parameter	Parameter Variation (%)	Time instant (s)
L_s	15	8
L_r	15	10
R_s	20	12
R_r	25	15

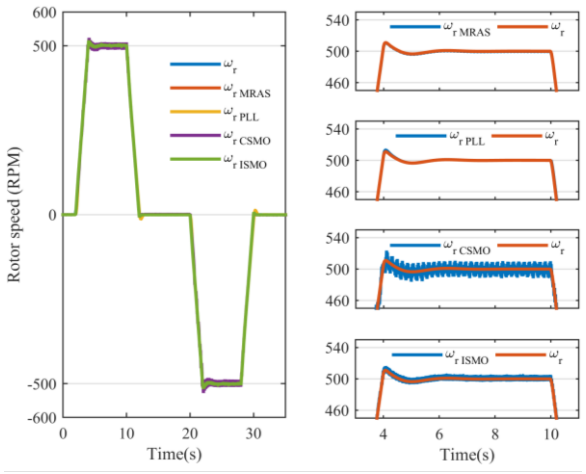

Fig. 6. Rotor speed estimation for different speed levels.

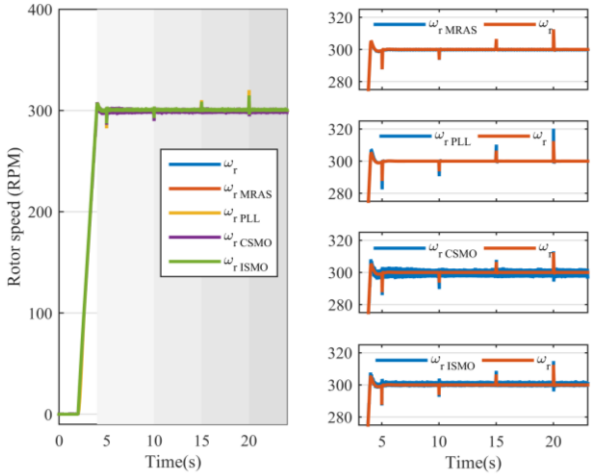

Fig. 7. Rotor speed estimation with motor load changes

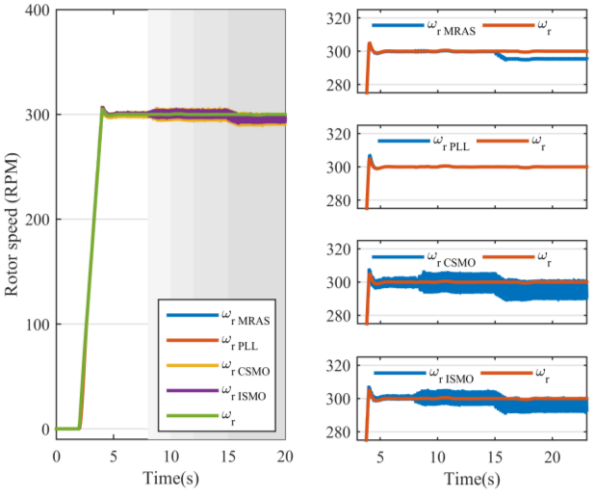

Fig. 8. Rotor speed estimation for parameters variation as Table II

VI. Experimental Analysis

The experimental verification of sensorless techniques and IFOC approach is carried out using an IGBT inverter drive. The main modules of the drive system are: SKKH 42/08E rectifier; SKM75GB063D IGBT inverter; and, 4700µF capacitance DC link. Hall effect sensors are used for current and voltage measurements: LA55-P current sensor; and, LV25-600 voltage sensor. The TMS320F28069 digital signal processor is used for IFOC control and sensorless implementation. As in numerical analysis, the experimental IFOC closed loop control uses the rotor speed estimation in all implementations. The DSP includes a 32 bit floating point core, 16bit-16ch-PWM generator and 12bit-3MSPS-12ch ADC converter. The rotor speed is measured using an AC58-12bit absolute encoder with gray code output. Through a DAC converter from the DSP variables, a DPO4034 oscilloscope captures the real and estimated speed. A 4 HP permanent magnet synchronous generator with resistive loads is used for motor load.

The experimental results obtained including rotor speed estimation techniques show similar behavior to the numerical analysis concerning the precision to speed estimation. The PLL technique presents less overall error. However, the Sliding Mode techniques presents lower ripple in the speed estimation when compared to numerical ones. Moreover, the ISMO results presents lower absolute error compared with CSMO results.

The drive behavior with different speed levels is analyzed in Fig. 9. The rotor speed is increased from 300 RPM to 500 RPM then it decreases from 500 RPM to 200 RPM. As it can be seen in Fig. 9b, the PLL technique presents lower drifts for all speed range. The MRAS approach Fig. 9a includes significant ripple in estimated speed and SMOs Fig. 9c and Fig. 9d presents drifts as the speed increases.

(a)

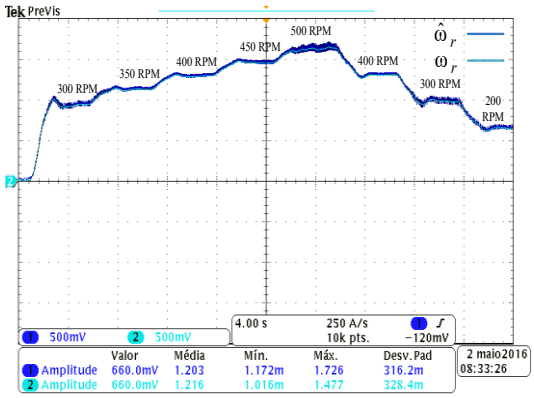

(b)

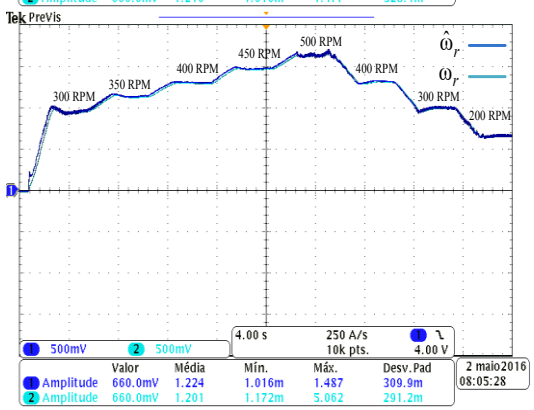

(c)

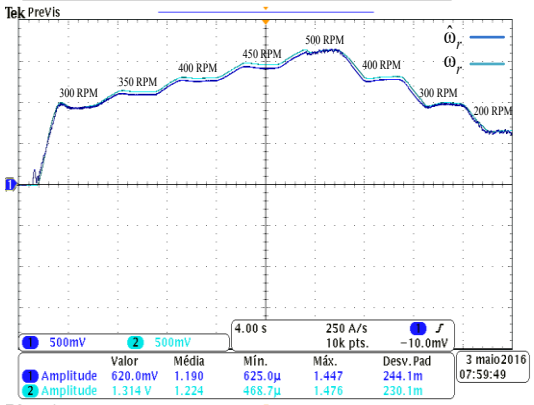

(d)

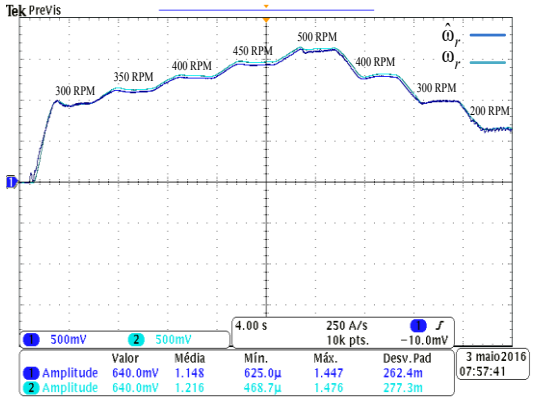

Fig. 9. Speed measurement and speed estimate with speed variation: (a) MRAS, (b) PLL (c) CSMO and (d) ISMO.

Figure 10 shows the performance of the speed estimation observers with load changes. The motor starts without load and at 20s a 5 Nm load is inserted. At 40s the load is changed to 7.5 Nm load. At 60s and 80s, the load is reduced to 5Nm and zero, respectively. The MRAS scheme shows the largest absolute error and increased ripple when compared to sliding mode observers, while PLL presents better performance and no ripple in the estimated speed.

(a)

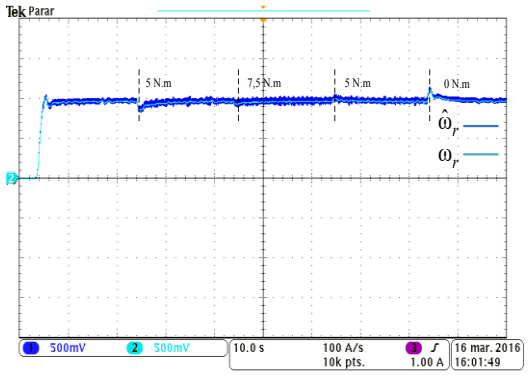

(b)

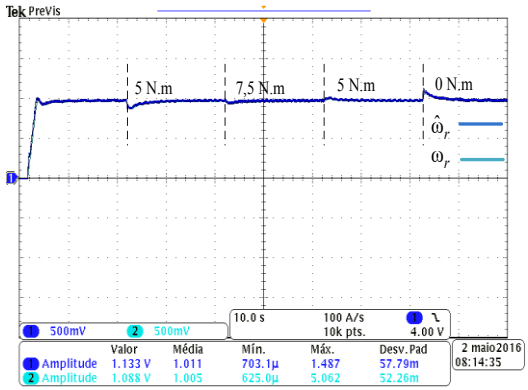

(c)

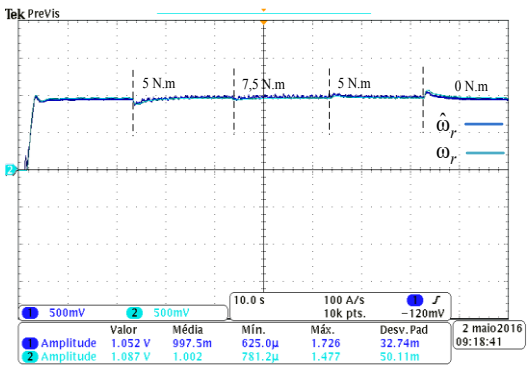

(d)

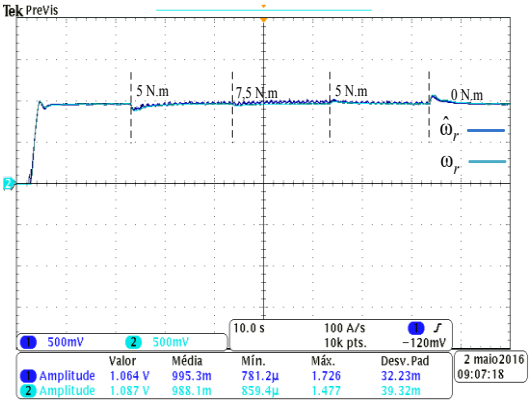

Fig. 10. Speed measurement and estimate with load changes (a) MRAS, (b) PLL, (c) CSMO and (d) ISMO.

VII. CONCLUSION

This paper presents an analysis on state of art high performance speed estimation techniques for induction motors drives. It presents concepts and design guidelines for numerical and experimental implementation of the discussed estimation approaches. In addition, the dynamic performance is evaluated for speed and load variations.

Numerical and experimental results show that the estimation techniques based on parametric dependency suffer considerable influence of the motor load, e.g. MRAS. Moreover, high ripple in speed estimation is present in all cases of MRAS experimental verification. The sliding mode based techniques presents better results, but some ripple is still present in the estimated speed. To reduce ripple in experimental implementations, the nonlinear functions of sliding mode observers are replaced by linear function with variable band. Even with its parametric dependence, the improved sliding mode observer (ISMO) presented slightly better response than the conventional one (CSMO). However, parametric variation affects both techniques, mostly changes in stator and rotor resistances. The PLL approach presents better results in all cases due to no parametric dependence algorithm. This concept also can be applied to avoid parametric dependence in IFOC control, as in slip computation. The numerical and experimental results show the effective robustness of PLL approach as for motor parameter variation as for different load and speed profiles.

REFERENCES

[1] P. Castaldi, W. Geri, M. Montanari e A. Tilli, *A new adaptive approach for on-line parameter and state estimation of induction motors,* Control Engineering Practice, 2005.

[2] A. Consoli, G. Scarcell e A. Testa, "Sensorless Control of AC Motors at Zero Speed," *Industrial Electronics ISIE '99. Proceedings of the IEEE International Symposium on*, 1999.

[3] J. Holtz, "Sensorless Control of Induction Motor Drives," *IEEE,* Aug. 2002.

[4] C. Schauder, "Adaptative Speed Identification for Vector Control of Induction Motors without Rotational Transducers," *IEEE Transactions on Industry Applications,* vol. 28, nº 1054-1061, pp. 1054-1061, Sep. 1992.

[5] Y. Guo, L. Huang, Y. Qiu e M. Maramatsu, "Inertia Identification and Auto-Tuning of Induction Motor Using MRAS," *3rd Power Electronics and Motion Control Conference,* pp. 1006-1010, 2000.

[6] F.-Z. Peng, "Robust Speed Identification for Speed-Sensorless Vector Control of Induction Motors," *IEEE TRANSCTIONS ON INDUSTRY APPLICATONS,* vol. 30, Sep.1994.

[7] T. Orlowska-Kowalska e M. Dybkowski, "Stator-Current-Based MRAS Estimator for a Wide Range Speed-Sensorless Induction-Motor Drive," *IEEE Transactions on Industrial Electronics ,* pp. 1296-1308, v.57, n.4 April 2010.

[8] M. Gayathri, D. Giaouris e J. Finch, "Performance Enhancement of Vector Controlled Drive with Rotor Flux Based MRAS Rotor Resistance Estimator," *International Conference on Computer Communication and Informatics*, 978-1-4577-1583-9, 2012.

[9] A. De Glória, D. Grosso, M. Olivieri e G. Restani, "A Novel Stability Analysis of PLL for Timing Recovery in Hard Disk Drives," *IEEE Transactions on Circuits and Systems - Fundamental Theory and Applications,* vol. 46, nº 8, pp. 1026-1031, 1999.

[10] M. Lai, M. Nakano e G. Hsieh, "Application Fuzzy Logic in the Phase-Locked Loop Speed Control of Induction Motor Drive," *IEEE Transactions on Industrial Electronics,* vol. 43, nº 6, pp. 630-639, 1996.

[11] L. Ran e Z. Guangzhou, "Position Sensorless Control for PMSM Using Sliding Mode Observer and Phase-Locked Loop," em *IEEE Power Electronics and Motion Control Conference*, 2009.

[12] L. Harnefors e H.-P. Nee, "A General Algorithm for Speed and Position Estimation of AC Motors," *IEEE Transactions on Industrial Electronics ,* vol. 47, nº 1, pp. 77-83, Feb. 2000.

[13] M. Comanescu e L. Xu, "An Improved Flux Observer Based on PLL Frequency Estimator for Sensorless Vector Control of Induction Motors," *IEEE Transactions on Industrial Electronics,* vol. 53, nº 1, pp. 50-56, Feb. 2006.

[14] Z. Peixoto, "Aplication of Sliding Mode Observers for Induced EMF, Position and Speed Estimation of Permanent Magnet Motors", *Power Electronics and Drive Systems-PEDS'95*, Cingapura, 1995.

[15] A. Sabanovic e D. B. Izosimov, "Aplications of Sliding Modes to Induction Motor Control," *IEEE Transactions on Industry Applications ,* pp. 41-49, n.1 Jan. 1981.

[16] J. Slotine, "On Sliding Observers for Nonlinear Systems," *Journal of Dynamics Systems, Measurement and Control*, vol. 109, 1987.

[17] V. Utkin, "Variable Structure Systems with Sliding Modes," *IEEE Transactions on Automatic Control ,* vol. 22, nº 2, pp. 212-222, Apr. 1977.

[18] V. Utkin, J. Guldner e M. Shijun, "Sliding Mode Control in Electro-Mechanical Systems," *IEEE Decision and Control Conference,* pp. 4591-4596, 1996.

[19] D. Souza, W. C. Aragão Filho e G. C. Sousa, "Adaptative Fuzzy Controller for Efficiency Optimization of Induction Motors," *IEEE Transactions On Industrial Electronics,* pp. 2157-2164, Aug. 2007.

[20] M. Eskola, *Speed and Postion Magnet Synchronous Motor in Matrix Converter and Voltage Source Converter Applications,* Tampare: Tampare University of Technology - PhD Thesis, 2006.